

Limit on the $B^0 \rightarrow \rho^0 \rho^0$ Branching Fraction and Implications for the CKM Angle α

- B. Aubert,¹ R. Barate,¹ D. Boutigny,¹ F. Couderc,¹ Y. Karyotakis,¹ J. P. Lees,¹ V. Poireau,¹ V. Tisserand,¹
A. Zghiche,¹ E. Grauges-Pous,² A. Palano,³ A. Pompili,³ J. C. Chen,⁴ N. D. Qi,⁴ G. Rong,⁴ P. Wang,⁴ Y. S. Zhu,⁴
G. Eigen,⁵ I. Ofte,⁵ B. Stugu,⁵ G. S. Abrams,⁶ A. W. Borgland,⁶ A. B. Breon,⁶ D. N. Brown,⁶ J. Button-Shafer,⁶
R. N. Cahn,⁶ E. Charles,⁶ C. T. Day,⁶ M. S. Gill,⁶ A. V. Gritsan,⁶ Y. Groysman,⁶ R. G. Jacobsen,⁶ R. W. Kadel,⁶
J. Kadyk,⁶ L. T. Kerth,⁶ Yu. G. Kolomensky,⁶ G. Kukartsev,⁶ G. Lynch,⁶ L. M. Mir,⁶ P. J. Oddone,⁶
T. J. Orimoto,⁶ M. Pripstein,⁶ N. A. Roe,⁶ M. T. Ronan,⁶ W. A. Wenzel,⁶ M. Barrett,⁷ K. E. Ford,⁷
T. J. Harrison,⁷ A. J. Hart,⁷ C. M. Hawkes,⁷ S. E. Morgan,⁷ A. T. Watson,⁷ M. Fritsch,⁸ K. Goetzen,⁸ T. Held,⁸
H. Koch,⁸ B. Lewandowski,⁸ M. Pelizaeus,⁸ K. Peters,⁸ T. Schroeder,⁸ M. Steinke,⁸ J. T. Boyd,⁹ J. P. Burke,⁹
N. Chevalier,⁹ W. N. Cottingham,⁹ M. P. Kelly,⁹ T. E. Latham,⁹ F. F. Wilson,⁹ T. Cuhadar-Donszelmann,¹⁰
C. Hearty,¹⁰ N. S. Knecht,¹⁰ T. S. Mattison,¹⁰ J. A. McKenna,¹⁰ D. Thiessen,¹⁰ A. Khan,¹¹ P. Kyberd,¹¹
L. Teodorescu,¹¹ A. E. Blinov,¹² V. E. Blinov,¹² V. P. Druzhinin,¹² V. B. Golubev,¹² V. N. Ivanchenko,¹²
E. A. Kravchenko,¹² A. P. Onuchin,¹² S. I. Serednyakov,¹² Yu. I. Skovpen,¹² E. P. Solodov,¹² A. N. Yushkov,¹²
D. Best,¹³ M. Bruinsma,¹³ M. Chao,¹³ I. Eschrich,¹³ D. Kirkby,¹³ A. J. Lankford,¹³ M. Mandelkern,¹³
R. K. Mommsen,¹³ W. Roethel,¹³ D. P. Stoker,¹³ C. Buchanan,¹⁴ B. L. Hartfiel,¹⁴ A. J. R. Weinstein,¹⁴
S. D. Foulkes,¹⁵ J. W. Gary,¹⁵ O. Long,¹⁵ B. C. Shen,¹⁵ K. Wang,¹⁵ D. del Re,¹⁶ H. K. Hadavand,¹⁶ E. J. Hill,¹⁶
D. B. MacFarlane,¹⁶ H. P. Paar,¹⁶ Sh. Rahatlou,¹⁶ V. Sharma,¹⁶ J. W. Berryhill,¹⁷ C. Campagnari,¹⁷ A. Cunha,¹⁷
B. Dahmes,¹⁷ T. M. Hong,¹⁷ A. Lu,¹⁷ M. A. Mazur,¹⁷ J. D. Richman,¹⁷ W. Verkerke,¹⁷ T. W. Beck,¹⁸
A. M. Eisner,¹⁸ C. J. Flacco,¹⁸ C. A. Heusch,¹⁸ J. Kroeseberg,¹⁸ W. S. Lockman,¹⁸ G. Nesom,¹⁸ T. Schalk,¹⁸
B. A. Schumm,¹⁸ A. Seiden,¹⁸ P. Spradlin,¹⁸ D. C. Williams,¹⁸ M. G. Wilson,¹⁸ J. Albert,¹⁹ E. Chen,¹⁹
G. P. Dubois-Felsmann,¹⁹ A. Dvoretskii,¹⁹ D. G. Hitlin,¹⁹ I. Narsky,¹⁹ T. Piatenko,¹⁹ F. C. Porter,¹⁹ A. Ryd,¹⁹
A. Samuel,¹⁹ S. Yang,¹⁹ S. Jayatilleke,²⁰ G. Mancinelli,²⁰ B. T. Meadows,²⁰ M. D. Sokoloff,²⁰ F. Blanc,²¹
P. Bloom,²¹ S. Chen,²¹ W. T. Ford,²¹ U. Nauenberg,²¹ A. Olivas,²¹ P. Rankin,²¹ W. O. Ruddick,²¹ J. G. Smith,²¹
K. A. Ulmer,²¹ J. Zhang,²¹ L. Zhang,²¹ A. Chen,²² E. A. Eckhart,²² J. L. Harton,²² A. Soffer,²² W. H. Toki,²²
R. J. Wilson,²² Q. Zeng,²² B. Spaan,²³ D. Altenburg,²⁴ T. Brandt,²⁴ J. Brose,²⁴ M. Dickopp,²⁴ E. Feltresi,²⁴
A. Hauke,²⁴ H. M. Lacker,²⁴ E. Maly,²⁴ R. Nogowski,²⁴ S. Otto,²⁴ A. Petzold,²⁴ G. Schott,²⁴ J. Schubert,²⁴
K. R. Schubert,²⁴ R. Schwierz,²⁴ J. E. Sundermann,²⁴ D. Bernard,²⁵ G. R. Bonneau,²⁵ P. Grenier,²⁵
S. Schrenk,²⁵ Ch. Thiebaux,²⁵ G. Vasileiadis,²⁵ M. Verderi,²⁵ D. J. Bard,²⁶ P. J. Clark,²⁶ F. Muheim,²⁶
S. Playfer,²⁶ Y. Xie,²⁶ M. Andreotti,²⁷ V. Azzolini,²⁷ D. Bettoni,²⁷ C. Bozzi,²⁷ R. Calabrese,²⁷ G. Cibinetto,²⁷
E. Luppi,²⁷ M. Negrini,²⁷ L. Piemontese,²⁷ A. Sarti,²⁷ F. Anulli,²⁸ R. Baldini-Ferroli,²⁸ A. Calcaterra,²⁸ R. de
Sangro,²⁸ G. Finocchiaro,²⁸ P. Patteri,²⁸ I. M. Peruzzi,²⁸ M. Piccolo,²⁸ A. Zallo,²⁸ A. Buzzo,²⁹ R. Capra,²⁹
R. Contri,²⁹ G. Crosetti,²⁹ M. Lo Vetere,²⁹ M. Macri,²⁹ M. R. Monge,²⁹ S. Passaggio,²⁹ C. Patrignani,²⁹
E. Robutti,²⁹ A. Santroni,²⁹ S. Tosi,²⁹ S. Bailey,³⁰ G. Brandenburg,³⁰ K. S. Chaisanguanthum,³⁰ M. Morii,³⁰
E. Won,³⁰ R. S. Dubitzky,³¹ U. Langenegger,³¹ J. Marks,³¹ U. Uwer,³¹ W. Bhimji,³² D. A. Bowerman,³²
P. D. Dauncey,³² U. Egede,³² J. R. Gaillard,³² G. W. Morton,³² J. A. Nash,³² M. B. Nikolich,³² G. P. Taylor,³²
M. J. Charles,³³ G. J. Grenier,³³ U. Mallik,³³ A. K. Mohapatra,³³ J. Cochran,³⁴ H. B. Crawley,³⁴ J. Lamsa,³⁴
W. T. Meyer,³⁴ S. Prell,³⁴ E. I. Rosenberg,³⁴ A. E. Rubin,³⁴ J. Yi,³⁴ N. Arnaud,³⁵ M. Davier,³⁵ X. Giroux,³⁵
G. Grosdidier,³⁵ A. Höcker,³⁵ F. Le Diberder,³⁵ V. Lepeltier,³⁵ A. M. Lutz,³⁵ T. C. Petersen,³⁵ M. Pierini,³⁵
S. Plaszczynski,³⁵ M. H. Schune,³⁵ G. Wormser,³⁵ C. H. Cheng,³⁶ D. J. Lange,³⁶ M. C. Simani,³⁶ D. M. Wright,³⁶
A. J. Bevan,³⁷ C. A. Chavez,³⁷ J. P. Coleman,³⁷ I. J. Forster,³⁷ J. R. Fry,³⁷ E. Gabathuler,³⁷ R. Gamet,³⁷
D. E. Hutchcroft,³⁷ R. J. Parry,³⁷ D. J. Payne,³⁷ C. Touramanis,³⁷ C. M. Cormack,³⁸ F. Di Lodovico,³⁸
C. L. Brown,³⁹ G. Cowan,³⁹ R. L. Flack,³⁹ H. U. Flaecher,³⁹ M. G. Green,³⁹ P. S. Jackson,³⁹ T. R. McMahon,³⁹
S. Ricciardi,³⁹ F. Salvatore,³⁹ M. A. Winter,³⁹ D. Brown,⁴⁰ C. L. Davis,⁴⁰ J. Allison,⁴¹ N. R. Barlow,⁴¹
R. J. Barlow,⁴¹ M. C. Hodgkinson,⁴¹ G. D. Lafferty,⁴¹ M. T. Naisbit,⁴¹ J. C. Williams,⁴¹ C. Chen,⁴² A. Farbin,⁴²
W. D. Hulsbergen,⁴² A. Jawahery,⁴² D. Kovalskyi,⁴² C. K. Lae,⁴² V. Lillard,⁴² D. A. Roberts,⁴² G. Blaylock,⁴³
C. Dallapiccola,⁴³ S. S. Hertzbach,⁴³ R. Kofler,⁴³ V. B. Koptchev,⁴³ T. B. Moore,⁴³ S. Saremi,⁴³ H. Staengle,⁴³

S. Willocq,⁴³ R. Cowan,⁴⁴ K. Koeneke,⁴⁴ G. Sciolla,⁴⁴ S. J. Sekula,⁴⁴ F. Taylor,⁴⁴ R. K. Yamamoto,⁴⁴ P. M. Patel,⁴⁵ S. H. Robertson,⁴⁵ A. Lazzaro,⁴⁶ V. Lombardo,⁴⁶ F. Palombo,⁴⁶ J. M. Bauer,⁴⁷ L. Cremaldi,⁴⁷ V. Eschenburg,⁴⁷ R. Godang,⁴⁷ R. Kroeger,⁴⁷ J. Reidy,⁴⁷ D. A. Sanders,⁴⁷ D. J. Summers,⁴⁷ H. W. Zhao,⁴⁷ S. Brunet,⁴⁸ D. Côté,⁴⁸ P. Taras,⁴⁸ H. Nicholson,⁴⁹ N. Cavallo,^{50,*} F. Fabozzi,^{50,*} C. Gatto,⁵⁰ L. Lista,⁵⁰ D. Monorchio,⁵⁰ P. Paolucci,⁵⁰ D. Piccolo,⁵⁰ C. Sciacca,⁵⁰ M. Baak,⁵¹ H. Bulten,⁵¹ G. Raven,⁵¹ H. L. Snoek,⁵¹ L. Wilden,⁵¹ C. P. Jessop,⁵² J. M. LoSecco,⁵² T. Allmendinger,⁵³ G. Benelli,⁵³ K. K. Gan,⁵³ K. Honscheid,⁵³ D. Hufnagel,⁵³ H. Kagan,⁵³ R. Kass,⁵³ T. Pulliam,⁵³ A. M. Rahimi,⁵³ R. Ter-Antonyan,⁵³ Q. K. Wong,⁵³ J. Brau,⁵⁴ R. Frey,⁵⁴ O. Igonkina,⁵⁴ M. Lu,⁵⁴ C. T. Potter,⁵⁴ N. B. Sinev,⁵⁴ D. Strom,⁵⁴ E. Torrence,⁵⁴ F. Coleccchia,⁵⁵ A. Dorigo,⁵⁵ F. Galeazzi,⁵⁵ M. Margoni,⁵⁵ M. Morandin,⁵⁵ M. Posocco,⁵⁵ M. Rotondo,⁵⁵ F. Simonetto,⁵⁵ R. Stroili,⁵⁵ C. Voci,⁵⁵ M. Benayoun,⁵⁶ H. Briand,⁵⁶ J. Chauveau,⁵⁶ P. David,⁵⁶ L. Del Buono,⁵⁶ Ch. de la Vaissière,⁵⁶ O. Hamon,⁵⁶ M. J. J. John,⁵⁶ Ph. Leruste,⁵⁶ J. Malclès,⁵⁶ J. Ocariz,⁵⁶ L. Roos,⁵⁶ G. Therin,⁵⁶ P. K. Behera,⁵⁷ L. Gladney,⁵⁷ Q. H. Guo,⁵⁷ J. Panetta,⁵⁷ M. Biasini,⁵⁸ R. Covarelli,⁵⁸ M. Pioppi,⁵⁸ C. Angelini,⁵⁹ G. Batignani,⁵⁹ S. Bettarini,⁵⁹ M. Bondioli,⁵⁹ F. Bucci,⁵⁹ G. Calderini,⁵⁹ M. Carpinelli,⁵⁹ F. Forti,⁵⁹ M. A. Giorgi,⁵⁹ A. Lusiani,⁵⁹ G. Marchiori,⁵⁹ M. Morganti,⁵⁹ N. Neri,⁵⁹ E. Paoloni,⁵⁹ M. Rama,⁵⁹ G. Rizzo,⁵⁹ G. Simi,⁵⁹ J. Walsh,⁵⁹ M. Haire,⁶⁰ D. Judd,⁶⁰ K. Paick,⁶⁰ D. E. Wagoner,⁶⁰ N. Danielson,⁶¹ P. Elmer,⁶¹ Y. P. Lau,⁶¹ C. Lu,⁶¹ V. Miftakov,⁶¹ J. Olsen,⁶¹ A. J. S. Smith,⁶¹ A. V. Telnov,⁶¹ F. Bellini,⁶² G. Cavoto,^{61,62} A. D'Orazio,⁶² E. Di Marco,⁶² R. Faccini,⁶² F. Ferrarotto,⁶² F. Ferroni,⁶² M. Gaspero,⁶² L. Li Gioi,⁶² M. A. Mazzoni,⁶² S. Morganti,⁶² G. Piredda,⁶² F. Polci,⁶² F. Safai Tehrani,⁶² C. Voeva,⁶² S. Christ,⁶³ H. Schröder,⁶³ G. Wagner,⁶³ R. Waldi,⁶³ T. Adye,⁶⁴ N. De Groot,⁶⁴ B. Franek,⁶⁴ G. P. Gopal,⁶⁴ E. O. Olaiya,⁶⁴ R. Aleksan,⁶⁵ S. Emery,⁶⁵ A. Gaidot,⁶⁵ S. F. Ganzhur,⁶⁵ P.-F. Giraud,⁶⁵ G. Graziani,⁶⁵ G. Hamel de Monchenault,⁶⁵ W. Kozanecki,⁶⁵ M. Legendre,⁶⁵ G. W. London,⁶⁵ B. Mayer,⁶⁵ G. Vasseur,⁶⁵ Ch. Yèche,⁶⁵ M. Zito,⁶⁵ M. V. Purohit,⁶⁶ A. W. Weidemann,⁶⁶ J. R. Wilson,⁶⁶ F. X. Yumiceva,⁶⁶ T. Abe,⁶⁷ D. Aston,⁶⁷ R. Bartoldus,⁶⁷ N. Berger,⁶⁷ A. M. Boyarski,⁶⁷ O. L. Buchmueller,⁶⁷ R. Claus,⁶⁷ M. R. Convery,⁶⁷ M. Cristinziani,⁶⁷ G. De Nardo,⁶⁷ J. C. Dingfelder,⁶⁷ D. Dong,⁶⁷ J. Dorfan,⁶⁷ D. Dujmic,⁶⁷ W. Dunwoodie,⁶⁷ S. Fan,⁶⁷ R. C. Field,⁶⁷ T. Glanzman,⁶⁷ S. J. Gowdy,⁶⁷ T. Hadig,⁶⁷ V. Halyo,⁶⁷ C. Hast,⁶⁷ T. Hryna'ova,⁶⁷ W. R. Innes,⁶⁷ M. H. Kelsey,⁶⁷ P. Kim,⁶⁷ M. L. Kocian,⁶⁷ D. W. G. S. Leith,⁶⁷ J. Libby,⁶⁷ S. Luitz,⁶⁷ V. Luth,⁶⁷ H. L. Lynch,⁶⁷ H. Marsiske,⁶⁷ R. Messner,⁶⁷ D. R. Muller,⁶⁷ C. P. O'Grady,⁶⁷ V. E. Ozcan,⁶⁷ A. Perazzo,⁶⁷ M. Perl,⁶⁷ B. N. Ratcliff,⁶⁷ A. Roodman,⁶⁷ A. A. Salnikov,⁶⁷ R. H. Schindler,⁶⁷ J. Schwiening,⁶⁷ A. Snyder,⁶⁷ A. Soha,⁶⁷ J. Stelzer,⁶⁷ J. Strube,^{54,67} D. Su,⁶⁷ M. K. Sullivan,⁶⁷ J. Va'vra,⁶⁷ S. R. Wagner,⁶⁷ M. Weaver,⁶⁷ W. J. Wisniewski,⁶⁷ M. Wittgen,⁶⁷ D. H. Wright,⁶⁷ A. K. Yarritu,⁶⁷ C. C. Young,⁶⁷ P. R. Burchat,⁶⁸ A. J. Edwards,⁶⁸ S. A. Majewski,⁶⁸ B. A. Petersen,⁶⁸ C. Roat,⁶⁸ M. Ahmed,⁶⁹ S. Ahmed,⁶⁹ M. S. Alam,⁶⁹ J. A. Ernst,⁶⁹ M. A. Saeed,⁶⁹ M. Saleem,⁶⁹ F. R. Wappler,⁶⁹ W. Bugg,⁷⁰ M. Krishnamurthy,⁷⁰ S. M. Spanier,⁷⁰ R. Eckmann,⁷¹ H. Kim,⁷¹ J. L. Ritchie,⁷¹ A. Satpathy,⁷¹ R. F. Schwitters,⁷¹ J. M. Izen,⁷² I. Kitayama,⁷² X. C. Lou,⁷² S. Ye,⁷² F. Bianchi,⁷³ M. Bona,⁷³ F. Gallo,⁷³ D. Gamba,⁷³ L. Bosisio,⁷⁴ C. Cartaro,⁷⁴ F. Cossutti,⁷⁴ G. Della Ricca,⁷⁴ S. Dittongo,⁷⁴ S. Grancagnolo,⁷⁴ L. Lanceri,⁷⁴ P. Poropat,^{74,†} L. Vitale,⁷⁴ G. Vuagnin,⁷⁴ F. Martinez-Vidal,^{2,75} R. S. Panvini,⁷⁶ Sw. Banerjee,⁷⁷ B. Bhuyan,⁷⁷ C. M. Brown,⁷⁷ D. Fortin,⁷⁷ K. Hamano,⁷⁷ P. D. Jackson,⁷⁷ R. Kowalewski,⁷⁷ J. M. Roney,⁷⁷ R. J. Sobie,⁷⁷ J. J. Back,⁷⁸ P. F. Harrison,⁷⁸ G. B. Mohanty,⁷⁸ H. R. Band,⁷⁹ X. Chen,⁷⁹ B. Cheng,⁷⁹ S. Dasu,⁷⁹ M. Datta,⁷⁹ A. M. Eichenbaum,⁷⁹ K. T. Flood,⁷⁹ M. Graham,⁷⁹ J. J. Hollar,⁷⁹ J. R. Johnson,⁷⁹ P. E. Kutter,⁷⁹ H. Li,⁷⁹ R. Liu,⁷⁹ A. Mihalyi,⁷⁹ Y. Pan,⁷⁹ R. Prepost,⁷⁹ P. Tan,⁷⁹ J. H. von Wimmersperg-Toeller,⁷⁹ J. Wu,⁷⁹ S. L. Wu,⁷⁹ Z. Yu,⁷⁹ M. G. Greene,⁸⁰ and H. Neal⁸⁰

(The BABAR Collaboration)

¹Laboratoire de Physique des Particules, F-74941 Annecy-le-Vieux, France

²IFAE, Universitat Autònoma de Barcelona, E-08193 Bellaterra, Barcelona, Spain

³Università di Bari, Dipartimento di Fisica and INFN, I-70126 Bari, Italy

⁴Institute of High Energy Physics, Beijing 100039, China

⁵University of Bergen, Inst. of Physics, N-5007 Bergen, Norway

⁶Lawrence Berkeley National Laboratory and University of California, Berkeley, California 94720, USA

⁷University of Birmingham, Birmingham, B15 2TT, United Kingdom

⁸Ruhr Universität Bochum, Institut für Experimentalphysik 1, D-44780 Bochum, Germany

⁹University of Bristol, Bristol BS8 1TL, United Kingdom

¹⁰University of British Columbia, Vancouver, British Columbia, Canada V6T 1Z1

¹¹Brunel University, Uxbridge, Middlesex UB8 3PH, United Kingdom

¹²Budker Institute of Nuclear Physics, Novosibirsk 630090, Russia

¹³University of California at Irvine, Irvine, California 92697, USA

¹⁴University of California at Los Angeles, Los Angeles, California 90024, USA

- ¹⁵University of California at Riverside, Riverside, California 92521, USA
¹⁶University of California at San Diego, La Jolla, California 92093, USA
¹⁷University of California at Santa Barbara, Santa Barbara, California 93106, USA
¹⁸University of California at Santa Cruz, Institute for Particle Physics, Santa Cruz, California 95064, USA
¹⁹California Institute of Technology, Pasadena, California 91125, USA
²⁰University of Cincinnati, Cincinnati, Ohio 45221, USA
²¹University of Colorado, Boulder, Colorado 80309, USA
²²Colorado State University, Fort Collins, Colorado 80523, USA
²³Universität Dortmund, Institut für Physik, D-44221 Dortmund, Germany
²⁴Technische Universität Dresden, Institut für Kern- und Teilchenphysik, D-01062 Dresden, Germany
²⁵Ecole Polytechnique, LLR, F-91128 Palaiseau, France
²⁶University of Edinburgh, Edinburgh EH9 3JZ, United Kingdom
²⁷Università di Ferrara, Dipartimento di Fisica and INFN, I-44100 Ferrara, Italy
²⁸Laboratori Nazionali di Frascati dell'INFN, I-00044 Frascati, Italy
²⁹Università di Genova, Dipartimento di Fisica and INFN, I-16146 Genova, Italy
³⁰Harvard University, Cambridge, Massachusetts 02138, USA
³¹Universität Heidelberg, Physikalisches Institut, Philosophenweg 12, D-69120 Heidelberg, Germany
³²Imperial College London, London, SW7 2AZ, United Kingdom
³³University of Iowa, Iowa City, Iowa 52242, USA
³⁴Iowa State University, Ames, Iowa 50011-3160, USA
³⁵Laboratoire de l'Accélérateur Linéaire, F-91898 Orsay, France
³⁶Lawrence Livermore National Laboratory, Livermore, California 94550, USA
³⁷University of Liverpool, Liverpool L69 7ZE, United Kingdom
³⁸Queen Mary, University of London, E1 4NS, United Kingdom
³⁹University of London, Royal Holloway and Bedford New College, Egham, Surrey TW20 0EX, United Kingdom
⁴⁰University of Louisville, Louisville, Kentucky 40292, USA
⁴¹University of Manchester, Manchester M13 9PL, United Kingdom
⁴²University of Maryland, College Park, Maryland 20742, USA
⁴³University of Massachusetts, Amherst, Massachusetts 01003, USA
⁴⁴Massachusetts Institute of Technology, Laboratory for Nuclear Science, Cambridge, Massachusetts 02139, USA
⁴⁵McGill University, Montréal, Quebec, Canada H3A 2T8
⁴⁶Università di Milano, Dipartimento di Fisica and INFN, I-20133 Milano, Italy
⁴⁷University of Mississippi, University, Mississippi 38677, USA
⁴⁸Université de Montréal, Laboratoire René J. A. Lévesque, Montréal, Quebec, Canada H3C 3J7
⁴⁹Mount Holyoke College, South Hadley, Massachusetts 01075, USA
⁵⁰Università di Napoli Federico II, Dipartimento di Scienze Fisiche and INFN, I-80126, Napoli, Italy
⁵¹NIKHEF, National Institute for Nuclear Physics and High Energy Physics, NL-1009 DB Amsterdam, The Netherlands
⁵²University of Notre Dame, Notre Dame, Indiana 46556, USA
⁵³Ohio State University, Columbus, Ohio 43210, USA
⁵⁴University of Oregon, Eugene, Oregon 97403, USA
⁵⁵Università di Padova, Dipartimento di Fisica and INFN, I-35131 Padova, Italy
⁵⁶Universités Paris VI et VII, Laboratoire de Physique Nucléaire et de Hautes Energies, F-75252 Paris, France
⁵⁷University of Pennsylvania, Philadelphia, Pennsylvania 19104, USA
⁵⁸Università di Perugia, Dipartimento di Fisica and INFN, I-06100 Perugia, Italy
⁵⁹Università di Pisa, Dipartimento di Fisica, Scuola Normale Superiore and INFN, I-56127 Pisa, Italy
⁶⁰Prairie View A&M University, Prairie View, Texas 77446, USA
⁶¹Princeton University, Princeton, New Jersey 08544, USA
⁶²Università di Roma La Sapienza, Dipartimento di Fisica and INFN, I-00185 Roma, Italy
⁶³Universität Rostock, D-18051 Rostock, Germany
⁶⁴Rutherford Appleton Laboratory, Chilton, Didcot, Oxon, OX11 0QX, United Kingdom
⁶⁵DSM/Dapnia, CEA/Saclay, F-91191 Gif-sur-Yvette, France
⁶⁶University of South Carolina, Columbia, South Carolina 29208, USA
⁶⁷Stanford Linear Accelerator Center, Stanford, California 94309, USA
⁶⁸Stanford University, Stanford, California 94305-4060, USA
⁶⁹State University of New York, Albany, New York 12222, USA
⁷⁰University of Tennessee, Knoxville, Tennessee 37996, USA
⁷¹University of Texas at Austin, Austin, Texas 78712, USA
⁷²University of Texas at Dallas, Richardson, Texas 75083, USA
⁷³Università di Torino, Dipartimento di Fisica Sperimentale and INFN, I-10125 Torino, Italy
⁷⁴Università di Trieste, Dipartimento di Fisica and INFN, I-34127 Trieste, Italy
⁷⁵IFIC, Universitat de Valencia-CSIC, E-46071 Valencia, Spain
⁷⁶Vanderbilt University, Nashville, Tennessee 37235, USA
⁷⁷University of Victoria, Victoria, British Columbia, Canada V8W 3P6
⁷⁸Department of Physics, University of Warwick, Coventry CV4 7AL, United Kingdom

⁷⁹University of Wisconsin, Madison, Wisconsin 53706, USA

⁸⁰Yale University, New Haven, Connecticut 06511, USA

(Dated: December 23, 2004)

We search for the decay $B^0 \rightarrow \rho^0 \rho^0$ in a data sample of about 227 million $\Upsilon(4S) \rightarrow B\bar{B}$ decays collected with the *BABAR* detector at the PEP-II asymmetric-energy e^+e^- collider at SLAC. We find no significant signal and set an upper limit of 1.1×10^{-6} at 90% CL on the branching fraction. As a result, the uncertainty due to penguin contributions on the CKM unitarity angle α measured in $B \rightarrow \rho\rho$ decays is 11° at 68% CL.

PACS numbers: 13.25.Hw, 11.30.Er, 12.15.Hh

Measurements of CP -violating asymmetries in the $B^0\bar{B}^0$ system provide tests of the standard model by over-constraining the Cabibbo-Kobayashi-Maskawa (CKM) quark-mixing matrix [1] through the measurement of the unitarity angles. Measuring the time-dependent CP asymmetry in a neutral- B -meson decay to a CP eigenstate dominated by the tree-level amplitude $b \rightarrow u\bar{d}$ gives an approximation α_{eff} to the CKM unitarity angle $\alpha \equiv \arg[-V_{td}V_{tb}^*/V_{ud}V_{ub}^*]$. The correction $\Delta\alpha = \alpha - \alpha_{\text{eff}}$, which accounts for the effects of penguin-amplitude contributions as an additional decay mechanism, can be extracted from an isospin analysis of the branching fractions of the B decays into the full set of isospin-related channels [2].

Measurements of branching fractions and time-dependent CP asymmetries in $B \rightarrow \pi\pi$, $\rho\pi$, and $\rho\rho$ have already provided information on α . Because the branching fraction for $B^0 \rightarrow \pi^0\pi^0$ is comparable to that for $B^+ \rightarrow \pi^+\pi^0$ and $B^0 \rightarrow \pi^+\pi^-$, the limit on the correction is weak: $|\Delta\alpha_{\pi\pi}| < 35^\circ$ at 90% confidence level (CL) [3]. (Charge conjugate B decay modes are implied in this paper.) In contrast, the $\rho^0\rho^0$ channel has a much smaller branching fraction than the channels with charged ρ 's [4, 5, 6, 7]. As a consequence, it is possible to set a tighter limit on $\Delta\alpha_{\rho\rho}$. This makes the $\rho\rho$ system particularly effective for measuring α in a model-independent way.

In $B \rightarrow \rho\rho$ decays the final state is a superposition of CP -odd and CP -even states, and an isospin-triangle relation [2] holds for each of the three helicity amplitudes, which can be separated through an angular analysis. The measured polarizations in $B^+ \rightarrow \rho^+\rho^0$ [4, 5] and $B^0 \rightarrow \rho^+\rho^-$ [6, 7] modes indicate that the ρ 's are nearly entirely longitudinally polarized. The current best limit on the $B^0 \rightarrow \rho^0\rho^0$ branching fraction was obtained by *BABAR* with a sample of 89 million $\Upsilon(4S) \rightarrow B\bar{B}$ decays [4].

In this Letter we present improved constraints on the $B^0 \rightarrow \rho^0\rho^0$ branching fraction and the penguin contribution to the measurement of the unitarity angle α . These results are based on data collected with the *BABAR* detector [8] at the PEP-II asymmetric-energy e^+e^- collider [9] located at the Stanford Linear Accelerator Center. A sample of 226.6 ± 2.5 million $B\bar{B}$ pairs, corresponding to an integrated luminosity of approximately 205 fb^{-1} , was recorded at the $\Upsilon(4S)$ resonance with

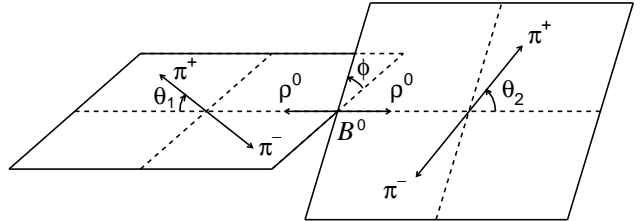


FIG. 1: Definition of helicity angles θ_1 , θ_2 , and ϕ for the decay $B^0 \rightarrow \rho^0 \rho^0$. The ρ^0 final states are shown in the ρ^0 rest frames.

the center-of-mass (c.m.) energy $\sqrt{s} = 10.58$ GeV. We use a sample of 16 fb^{-1} taken 40 MeV below the $\Upsilon(4S)$ resonance to study background contributions from $e^+e^- \rightarrow q\bar{q}$ ($q = u, d, s$, or c) continuum events.

To reconstruct $B^0 \rightarrow \rho^0 \rho^0 \rightarrow (\pi^+\pi^-)(\pi^+\pi^-)$ candidates, we select four charged tracks that are consistent with originating from a single vertex near the e^+e^- interaction point. Particle identification is provided by measurements of the energy loss in the silicon vertex tracker and the drift chamber and by the Cherenkov angle in an internally reflecting ring-imaging Cherenkov detector.

The angular distribution of the $B^0 \rightarrow \rho^0 \rho^0$ decay products can be expressed as a function of the helicity angles (θ_1 , θ_2 , ϕ), which are defined by the directions of the two-body ρ^0 decay axes and the direction opposite the B in the ρ^0 rest systems, as shown in Fig. 1. Since the detector acceptance does not depend on ϕ , the resulting angular distribution $d^2\Gamma/(\Gamma d\cos\theta_1 d\cos\theta_2)$ is

$$\frac{9}{4} \left\{ \frac{1}{4} (1 - f_L) \sin^2 \theta_1 \sin^2 \theta_2 + f_L \cos^2 \theta_1 \cos^2 \theta_2 \right\}, \quad (1)$$

where $f_L = |A_0|^2/(\Sigma|A_\lambda|^2)$ is the longitudinal polarization fraction and $A_{\lambda=-1,0,+1}$ are the helicity amplitudes.

The identification of signal B candidates is based on two kinematic variables: the beam-energy-substituted mass, $m_{\text{ES}} = [(s/2 + \mathbf{p}_i \cdot \mathbf{p}_B)^2/E_i^2 - \mathbf{p}_B^2]^{1/2}$, where the initial total e^+e^- four-momentum (E_i, \mathbf{p}_i) and the B momentum \mathbf{p}_B are defined in the laboratory frame; and the difference between the reconstructed B energy in the c.m. frame and its known value $\Delta E = E_B^{\text{cm}} - \sqrt{s}/2$. The signal m_{ES} and ΔE resolutions are $2.6 \text{ MeV}/c^2$ and 20 MeV ,

respectively. The selection requirements for m_{ES} , ΔE , the two $\pi^+\pi^-$ invariant masses $m_{1,2}$, and the helicity angles are the following: $5.24 < m_{\text{ES}} < 5.29 \text{ GeV}/c^2$, $|\Delta E| < 85 \text{ MeV}$, $0.55 < m_{1,2} < 1.00 \text{ GeV}/c^2$, and $|\cos \theta_{1,2}| < 0.99$. The latter requirement removes a region with low reconstruction efficiency.

To reject the dominant continuum background we require $|\cos \theta_T| < 0.8$, where θ_T is the angle between the B -candidate thrust axis and that of the remaining tracks and neutral clusters in the event, calculated in the c.m. frame. Other discriminating variables include the polar angles of the B momentum vector and the B -candidate thrust axis with respect to the beam axis in the c.m. frame, and the two Legendre moments L_0 and L_2 of the energy flow around the B -candidate thrust axis [10]. These variables are combined in a neural network, the output of which is transformed into a variable \mathcal{E} for which the signal and background distributions are approximately Gaussian.

We veto the background mode $B^0 \rightarrow D^-\pi^+ \rightarrow h^+\pi^-\pi^-\pi^+$, where h^+ refers to a pion or kaon. We require the invariant mass of the three-particle combination that excludes the highest-momentum track in the candidate B rest frame to be inconsistent with being the D -meson mass ($|m_{h\pi\pi} - m_D| > 13 \text{ MeV}/c^2$). After application of all selection criteria, $N_{\text{cand}} = 35740$ events are retained, most of which are background events with candidates in the sidebands of the variables. On average each selected event has 1.05 candidates. When more than one candidate is present in the same event, one candidate is selected randomly.

The signal selection efficiency determined from Monte Carlo (MC) [11] simulation is 27% or 32% for longitudinally or transversely polarized events, respectively. MC simulation shows that 22% of longitudinally and 8% of transversely polarized signal events are misreconstructed with one or more tracks not originating from the $B^0 \rightarrow \rho^0\rho^0$ decay. These are mostly due to combinatorial background from low-momentum tracks from the other B . We treat these as part of the signal.

Further background separation is achieved by the use of multivariate B -flavor-tagging algorithms trained to identify primary leptons, kaons, soft pions and high-momentum charged particles from the other B in the event [12]. The discrimination power arises from the difference between the tagging efficiencies for signal and background in the five tagging categories c_{tag} .

We use an unbinned extended maximum likelihood fit to extract the $B^0 \rightarrow \rho^0\rho^0$ event yield. The likelihood function is

$$\mathcal{L} = \exp \left(-\sum_k n_k \right) \prod_{i=1}^{N_{\text{cand}}} \left(\sum_j n_j \mathcal{P}_j(\vec{x}_i) \right), \quad (2)$$

where n_j is the number of events for each hypothesis j (signal, continuum, and six B -background classes),

and $\mathcal{P}_j(\vec{x}_i)$ is the corresponding probability density function (PDF), evaluated with the variables $\vec{x}_i = \{m_{\text{ES}}, \Delta E, \mathcal{E}, m_1, m_2, \cos \theta_1, \cos \theta_2, c_{\text{tag}}\}$ of the i th event.

We use MC-simulated events to study the background from other B decays. The charmless modes are grouped into five classes with similar kinematic and topological properties: $B^0 \rightarrow a_1^\pm \pi^\mp$; $B^0 \rightarrow \rho^0 K^{*0}$; $B^+ \rightarrow \rho^+ \rho^0$; a combination of $B \rightarrow \rho\pi$ and $B^0 \rightarrow \rho^+\rho^-$; and B decays to other charmless modes not included explicitly. One additional class accounts for the remaining neutral and charged B decays to charm modes. The number of events in each class n_j is left free in the fit with the exception of three classes where n_j is fixed either to the expectations from independent measurements (78 ± 20 events of $B^+ \rightarrow \rho^+ \rho^0$, and 48 ± 8 events of $B \rightarrow \rho\pi$ and $B^0 \rightarrow \rho^+\rho^-$) or to the extrapolation from the flavor-SU(3)-related B -decay modes [4] (25 ± 18 events of $B^0 \rightarrow \rho^0 K^{*0}$).

Since the correlations among the variables are found to be small, we take each \mathcal{P}_j as the product of the PDFs for the separate variables. Exceptions are the correlation between the two helicity angles in signal, and mass-helicity correlations in backgrounds and misreconstructed signal, taken into account as discussed below.

We use double-Gaussian functions to parameterize the m_{ES} and ΔE PDFs for signal, and a relativistic P -wave Breit-Wigner (BW) convoluted with a Gaussian resolution function for the resonance masses. The angular distribution for signal, expressed as a function of the longitudinal polarization in Eq. (1), is multiplied by a detector acceptance function $\mathcal{G}(\cos \theta_1, \cos \theta_2)$, obtained with MC simulation. The distributions of misreconstructed signal events are parameterized with empirical shapes in a fashion similar to that used for B background, as described below. The \mathcal{E} variable is described by two asymmetric Gaussian functions with different parameters for signal and background distributions.

The m_{ES} distribution of the continuum background is described with the ARGUS parameterization [13]. The ΔE and resonance mass $m_{1,2}$ PDFs are parameterized with low-degree polynomials. The parameterization of the m_1 and m_2 distributions includes a BW resonant component to account for the real ρ^0 resonances in the continuum background, which are assumed to be unpolarized and thus to have a flat distribution in $\cos \theta_{1,2}$. The $\cos \theta_{1,2}$ distribution of the continuum background excluding the real resonances is parameterized with a second-degree polynomial and an exponential function to allow for the increased fraction of combinatorial $\pi^+\pi^-$ candidates with low momentum pions near $|\cos \theta_{1,2}| = 1$. This parameterization depends on the ρ candidate's mass.

The PDFs for exclusive non-signal B decay modes are generally modeled with empirical non-parametric distributions [14]. However, analytical distributions are used for the variables that have distributions identical to those for signal, such as m_{ES} when all four tracks come from the same B , or $\pi^+\pi^-$ invariant mass $m_{1,2}$ when both

tracks come from a ρ^0 meson. The two ρ^0 candidates of some exclusive non-signal modes can have very different mass and helicity distributions. This occurs when one of the two ρ^0 candidates is real (e.g., $\rho^+ \rho^0$, $\rho^0 K^{*0}$) or when one of the two ρ^0 candidates contains a high-momentum pion ($a_1 \pi$). In such cases, we use a four-variable correlated mass-helicity PDF.

The signal and B -background PDF parameters are extracted from MC simulation while the continuum background PDF parameters are obtained from data in m_{ES} and ΔE sidebands. The MC parameters of m_{ES} , ΔE , and \mathcal{E} are adjusted by comparing data and MC in calibration channels with similar kinematics and topology, such as $B^0 \rightarrow D^- \pi^+$ with $D^- \rightarrow K^+ \pi^- \pi^-$. Finally, the B -flavor tagging PDFs for all categories are the discrete c_{tag} distributions of tagging efficiencies. Large samples of fully reconstructed B -meson decays are used to obtain the B -tagging efficiencies for signal B decays and to study systematic uncertainties in the MC values of B -tagging efficiencies for the B backgrounds.

Table I shows the results of the fit. No significant signal yield is observed. We obtain an upper limit by integrating the normalized likelihood distribution over the positive values of the branching fraction. The value of f_L is fixed to 1 in the fit, as this assumption has been shown to give the most conservative upper limit and it approximates the values obtained in the $B \rightarrow \rho\rho$ decays dominated by the tree-level amplitude. The statistical significance is taken as the square root of the change in $-2 \ln \mathcal{L}$ when the number of signal events is constrained to zero in the likelihood fit. In Fig. 2 we show the projections of the fit results onto m_{ES} and ΔE .

Systematic errors in the fit originate from uncertainties in the PDF parameterizations, which arise from the limited number of events in the sideband data and signal control samples. The PDF parameters are varied by their respective uncertainties to derive the corresponding systematic errors (6.0 events). The event yields from the B -background modes fixed in the fit are varied according to the uncertainties in the measured or estimated branching fractions. This results in a systematic error on the

TABLE I: Summary of results: signal yield (n_{sig}), selection efficiency (Eff), branching fraction (\mathcal{B}), branching fraction upper limit (UL) at 90% CL, and significance (including systematic uncertainties). The assumption $f_L = 1$ is used. The systematic errors are quoted last.

Quantity	Value
n_{sig} (events)	$33^{+22}_{-20} \pm 12$
Eff (%)	27.1 ± 1.3
$\mathcal{B} (\times 10^{-6})$	$0.54^{+0.36}_{-0.32} \pm 0.19$
UL ($\times 10^{-6}$)	1.1
Significance (σ)	1.6

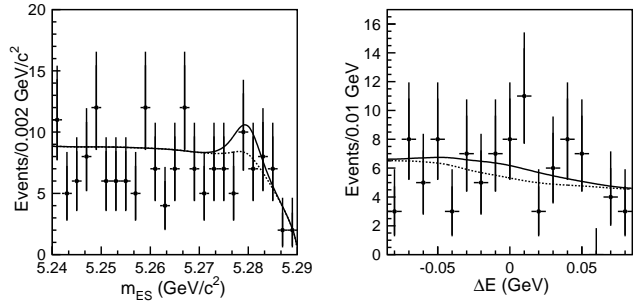


FIG. 2: Projections of the multidimensional fit onto m_{ES} and ΔE with a requirement on the signal-to-background probability ratio $\mathcal{P}_{\text{sig}}/\mathcal{P}_{\text{bkg}}$ with the plotted variable excluded. The histogram shows the data and the solid (dashed) line shows the full (background only) PDF projection. The projections contain 22.5% and 23.9% of signal, and less than 0.5% and 0.2% of continuum background, respectively.

signal yield of 5.8 events. We also assign a systematic error of 3.0 events to cover a possible fit bias, evaluated with MC experiments.

We estimate the systematic uncertainty due to signal- $a_1^\pm \pi^\mp$ interference using a simulation study in which the decay amplitudes for $B^0 \rightarrow \rho^0 \rho^0$ are generated according to this measurement and those for $B^0 \rightarrow a_1^\pm \pi^\mp$ correspond to a branching fraction of 4×10^{-5} [15]. The relative phases between these are modeled with BW amplitudes for all $\rho \rightarrow \pi\pi$ and $a_1 \rightarrow \rho\pi$ combinations, with additional constants. The values of the constants and the $a_1^\pm \pi^\mp$ CP asymmetries are varied over the allowed ranges. We take the rms variation of the average signal yield (7.5 events) as a systematic uncertainty.

Uncertainties in the reconstruction efficiency arise from track finding (3%), particle identification (2%), and other selection requirements, such as on vertex probability (2%), track multiplicity (1%), and thrust angle (1%).

Our measurement confirms the small value of the $B^0 \rightarrow \rho^0 \rho^0$ branching fraction with the statistical uncertainty improved by approximately a factor of two over our previous result [4]. Since the tree contribution to the $B^0 \rightarrow \rho^0 \rho^0$ decay is color-suppressed, the decay rate is sensitive to the penguin amplitude. Thus, this mode has important implications for constraining the uncertainty due to penguin contributions in the measurement of the CKM unitarity angle α with $B \rightarrow \rho\rho$ decays.

In the isospin analysis [2], we minimize a χ^2 that includes the measured quantities expressed as the lengths of the sides of the isospin triangles. We use the measured branching fractions and fractions of longitudinal polarization of the $B^+ \rightarrow \rho^+ \rho^0$ [4, 5] and $B^0 \rightarrow \rho^+ \rho^-$ [6, 7] decays, the CP -violating parameters S_L^{+-} and C_L^{+-} obtained from the time evolution of the longitudinally polarized $B^0 \rightarrow \rho^+ \rho^-$ decay [7], and the branching fraction of $B^0 \rightarrow \rho^0 \rho^0$ from this analysis. We neglect isospin-

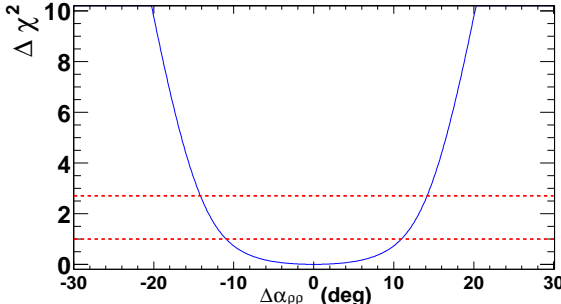


FIG. 3: $\Delta\chi^2$ on $\Delta\alpha_{\rho\rho}$ obtained from the isospin analysis discussed in the text. The dashed lines at $\Delta\chi^2 = 1$ and $\Delta\chi^2 = 2.7$ are taken for the 1σ (68%) and 1.64σ (90%) interval estimates.

breaking effects, non-resonant, and $I = 1$ isospin contributions [16].

With the $B^0 \rightarrow \rho^0 \rho^0$ measurement we improve the constraint on α due to the penguin contribution and obtain a 68% (90%) CL limit on $\Delta\alpha_{\rho\rho} = \alpha - \alpha_{\text{eff}}$ of $\pm 11^\circ$ ($\pm 14^\circ$). Fig. 3 shows the $\Delta\chi^2$ on $\Delta\alpha_{\rho\rho}$. Since the central value from Fig. 3 is $\Delta\alpha_{\rho\rho} = 0$, the central value of α obtained from the isospin analysis is the same as α_{eff} , which is constrained by the relation $\sin(2\alpha_{\text{eff}}) = S_L^{+-}/(1 - C_L^{+-})^{1/2}$ and is measured with the $B^0 \rightarrow \rho^+ \rho^-$ decay [7] to be $\alpha_{\text{eff}} = (102^{+16}_{-12}(\text{stat})^{+5}_{-4}(\text{syst}))^\circ$ at 68% CL, where the solution closest to the CKM best fit central value [17] is chosen.

The error due to the penguin contribution may become the dominant uncertainty in the measurement of α using $B \rightarrow \rho\rho$ decays. However, if $B^0 \rightarrow \rho^0 \rho^0$ decays are observed, time-dependent and angular analyses will allow us to measure the CP parameters S_L^{00} and C_L^{00} , analogous to S_L^{+-} and C_L^{+-} , resolving ambiguities inherent to isospin triangle orientations.

In summary, we have improved the precision on the measurement of the $B^0 \rightarrow \rho^0 \rho^0$ branching fraction by approximately a factor of two. The limit on this branching fraction relative to those for $B^+ \rightarrow \rho^0 \rho^+$ and $B^0 \rightarrow \rho^+ \rho^-$ provides a tight constraint on the penguin uncertainty in the determination of the CKM unitarity angle α . The results summarized in Table I supersede our previous measurement [4].

We are grateful for the excellent luminosity and machine conditions provided by our PEP-II colleagues, and for the substantial dedicated effort from the computing organizations that support *BABAR*. The collaborating institutions wish to thank SLAC for its support and kind hospitality. This work is supported by DOE and NSF (USA), NSERC (Canada), IHEP (China), CEA and CNRS-IN2P3 (France), BMBF and DFG (Germany), INFN (Italy), FOM (The Netherlands), NFR (Norway), MIST (Russia), and PPARC (United Kingdom). Individuals have received support from CONACyT (Mexico), A. P. Sloan Foundation, Research Corporation, and Alexander von Humboldt Foundation.

* Also with Università della Basilicata, Potenza, Italy

† Deceased

- [1] M. Kobayashi, T. Maskawa, Prog. Theor. Phys. **49**, 652 (1973); N. Cabibbo, Phys. Rev. Lett. **10**, 531 (1963).
- [2] M. Gronau, D. London, Phys. Rev. Lett. **65**, 3381 (1990).
- [3] *BABAR* Collaboration, B. Aubert *et al.*, hep-ex/0412037, submitted to Phys. Rev. Lett.
- [4] *BABAR* Collaboration, B. Aubert *et al.*, Phys. Rev. Lett. **91**, 171802 (2003).
- [5] Belle Collaboration, J. Zhang *et al.*, Phys. Rev. Lett. **91**, 221801 (2003).
- [6] *BABAR* Collaboration, B. Aubert *et al.*, Phys. Rev. D **69**, 031102 (2004).
- [7] *BABAR* Collaboration, B. Aubert *et al.*, Phys. Rev. Lett. **93**, 231801 (2004).
- [8] *BABAR* Collaboration, B. Aubert *et al.*, Nucl. Instrum. Methods Phys. Res., Sect. A **479**, 1 (2002).
- [9] PEP-II Conceptual Design Report, SLAC-R-418 (1993).
- [10] *BABAR* Collaboration, B. Aubert *et al.*, Phys. Rev. Lett. **89**, 281802 (2002); Phys. Rev. D **70**, 032006 (2004).
- [11] The *BABAR* detector Monte Carlo simulation is based on GEANT4: S. Agostinelli *et al.*, Nucl. Instrum. Methods Phys. Res., Sect. A **506**, 250 (2003).
- [12] *BABAR* Collaboration, B. Aubert *et al.*, Phys. Rev. Lett. **89**, 201802 (2003).
- [13] ARGUS Collaboration, H. Albrecht *et al.*, Z. Phys. C **48**, 543 (1990).
- [14] K.S. Cranmer, Comput. Phys. Commun. **136**, 198 (2001).
- [15] *BABAR* Collaboration, B. Aubert *et al.*, hep-ex/0408021.
- [16] A.F. Falk *et al.*, Phys. Rev. D **69**, 011502 (2004).
- [17] J. Charles *et al.*, hep-ph/0406184, submitted to Eur. Phys. J. C; M. Bona *et al.*, hep-ph/0408079.